Electronic Supplementary Material (ESI) for ChemComm.
This journal is © The Royal Society of Chemistry 2019

Electronic Supplementary Information (ESI)

Achieving high-efficiency purely organic room-temperature phosphorescence from boronic ester substitution of phenoxathiine

Mengke Li,[a†] Xinyi Cai,[a†] Zhenyang Qiao,[a] Kunkun Liu,[a, b] Wentao Xie,[a] Liangying Wang,[a] Nan Zheng,[a] and Shi-Jian Su[a]*

[a.] State Key Laboratory of Luminescent Materials and Devices, Institute of Polymer Optoelectronic Materials and Devices, South China University of Technology, Guangzhou 510640, P. R. China.
† These authors contribute equally to this work.
[b.] South China Institute of Collaborative Innovation, Dongguan 523808, China
E-mail: mssjsu@scut.edu.cn.

Contents

1. Reported RTP structures

Table S1. Reported RTP structures and their corresponding phosphorescence efficiencies (ϕ_P).

Molecular structures with low ϕ_P

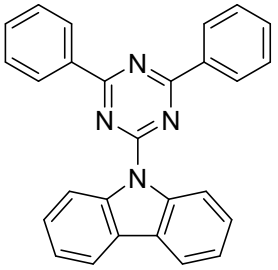

ϕ_P=1.25%

Nat. Mater., **2015**, 14, 685.

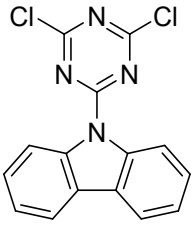

ϕ_P=2.1%

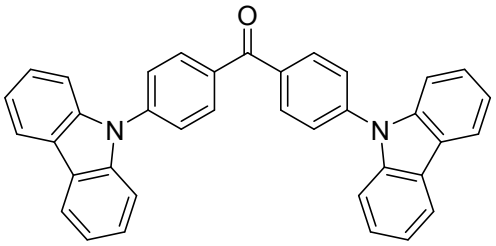

ϕ_P=1.0%

Adv. Opt. Mater., **2015**, 3, 1184.

Molecular structures with medium ϕ_P

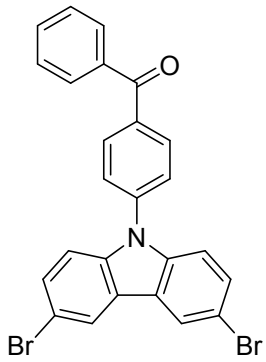

ϕ_P=7.5%

Adv. Mater., **2015**, 27, 6195.

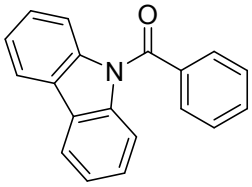

ϕ_P=5.0%

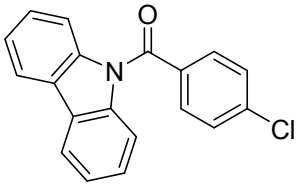

ϕ_P=3.2%

Adv. Mater., **2017**, 29, 1701244.

Molecular structures with high ϕ_P

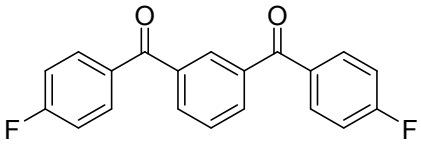

ϕ_P=17.7%

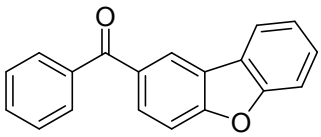

ϕ_P=34.5%

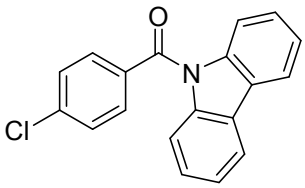

ϕ_P=36%

Chem, **2016**, 1, 592.

Arylboronic esters (with low ϕ_P)

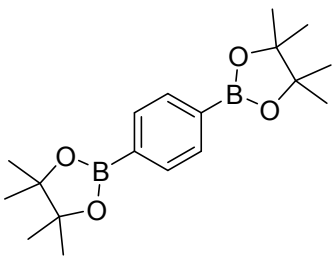

ϕ_P=2%

J. Am. Chem. Soc., **2017**, 139, 2728-2733.

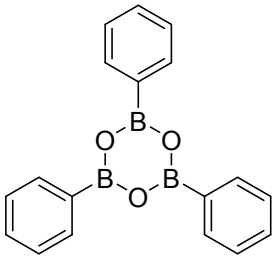

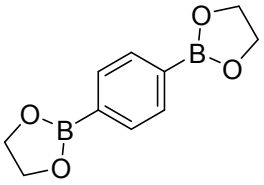

ChemPhotoChem, **2017**, 1, 102-106.

2. Experimental Procedures

2.1 General Information

All of the compounds were dissolved in deuterated chloroform ($CDCl_3$) solution to measure ^1H and ^{13}C NMR spectra with a Bruker NMR spectrometer. Also, mass spectra were measured in THF solutions with a JEOL JMS-K9 mass spectrometer to confirm their molecular weight. Thermogravimetric analyses (TGA) were measured on Netzsch TG 209 under nitrogen flow with a heating rate of 10 ℃/min. Differential scanning calorimetry (DSC) analyses were measured on Netzsch DSC 209 under nitrogen flow with a heating rate of 10 ℃/min and a cooling rate of 20 ℃/min. Ultraviolet-visible (UV-vis) absorption and photoluminescence (PL) spectra were measured with Perkin-Elmer Lambda 950-PKA UV/vis and FluoroMax-4 spectrofluorometer, respectively. PL quantum yields (PLQYs) of all crystals were measured with HAMAMATSU absolute PL quantum yield spectrometer (C11347). Transient PL lifetimes of the powder samples were measured using Quantaurus-Tau fluorescence lifetime measurement system (C11367-03, Hamamatsu Photonics Co., Japan). Transient PL spectra of all crystalline samples were measured with a transient lifetime spectrometer (FL980, Edinburgh Instrument). Temperature-dependent PL spectra of all crystals were recorded under Ar atmosphere using a transient lifetime spectrometer (FL980, Edinburgh Instrument).

2.2 Calculation of exciton dynamic rate constants

The radiative and non-radiative phosphorescence rate constants are calculated based on transient lifetime and photoluminescence quantum yield. The phosphorescence transient lifetime and the phosphorescence quantum yield at corresponding temperature can be expressed as:

$$\tau(T) = {}^{1}\!\Big/\!{}_{\left(k_p + k_{nr}(T)\right)}$$

$$\phi_P(T) = \phi_{ISC} k_p \tau(T)$$

where $\tau(T)$ is the phosphorescence transient lifetime at T, k_p is the phosphorescence rate constant, $k_{nr}(T)$ is nonradiative deactivation rate constant of T_1 state at T, and it is strongly dependent on temperature. $\phi_P(T)$ is phosphorescence quantum yield at T, ϕ_{ISC} is the intersystem crossing quantum yield from S_1 to T_1. It is believed that the non-radiative process is basically completely suppressed. So, the ϕ_{ISC} is determined by the phosphorescence quantum yield at 77 K.

2.3 Synthesis Routes

TE-BPin. Thianthrene was obtained from commercial sources. Without further purification, thianthrene (7 g) was dissolved with acetic acid (150 mL) and trichloromethane (40 mL), and then the mixture was added into a 250 mL flask. After the raw material was completely dissolved, liquid bromine (1.66 mL, ρ=3.119 g/mL) was added into the mixture dropwise. After stirring 30 minutes at room temperature, the mixture was heated up to 80 ℃ and reacted 24 hours at this temperature. When the reaction was finished, the resultant was poured into sodium bisulfite solution to remove non-reacted bromine. The final product (5.4 g) was obtained by extraction with dichloromethane, drying with anhydrous magnesium sulfate, solvent evaporation and purified by chromatographic column.

The product derived from the step forward was added into a 250 mL flask and cooled to -78 ℃, and then n-butyllithium (7.6 mL, 2.5 M) was added into the solution dropwise. After an hour, isopropoxyboronic acid pinacol ester (5.6 g) was added into the solution dropwise, and then the reaction was kept for 12 hours after stop cooling. The resultant was extracted with dichloromethane, drying with anhydrous magnesium sulfate, solvent evaporation and

purified by chromatographic column. ^{1}H NMR (500 MHz, $CDCl_3$) δ 7.91 (d, J = 1.0 Hz, 1H), 7.64 (dd, J = 7.7, 1.3 Hz, 1H), 7.48 – 7.45 (m, 3H), 7.23 (dd, J = 5.8, 3.4 Hz, 2H). ^{13}C NMR (126 MHz, $CDCl_3$) δ 139.04, 135.57, 135.19, 134.80, 133.79, 128.70, 128.06, 127.66, 84.10, 77.37 – 76.97, 76.97 – 76.92, 76.76, 24.81. Calcd ($C_{18}H_{19}BO_2S_2$): 342.28, APCI-MS (mass m/z); found: 342.3 ((M+1)+).

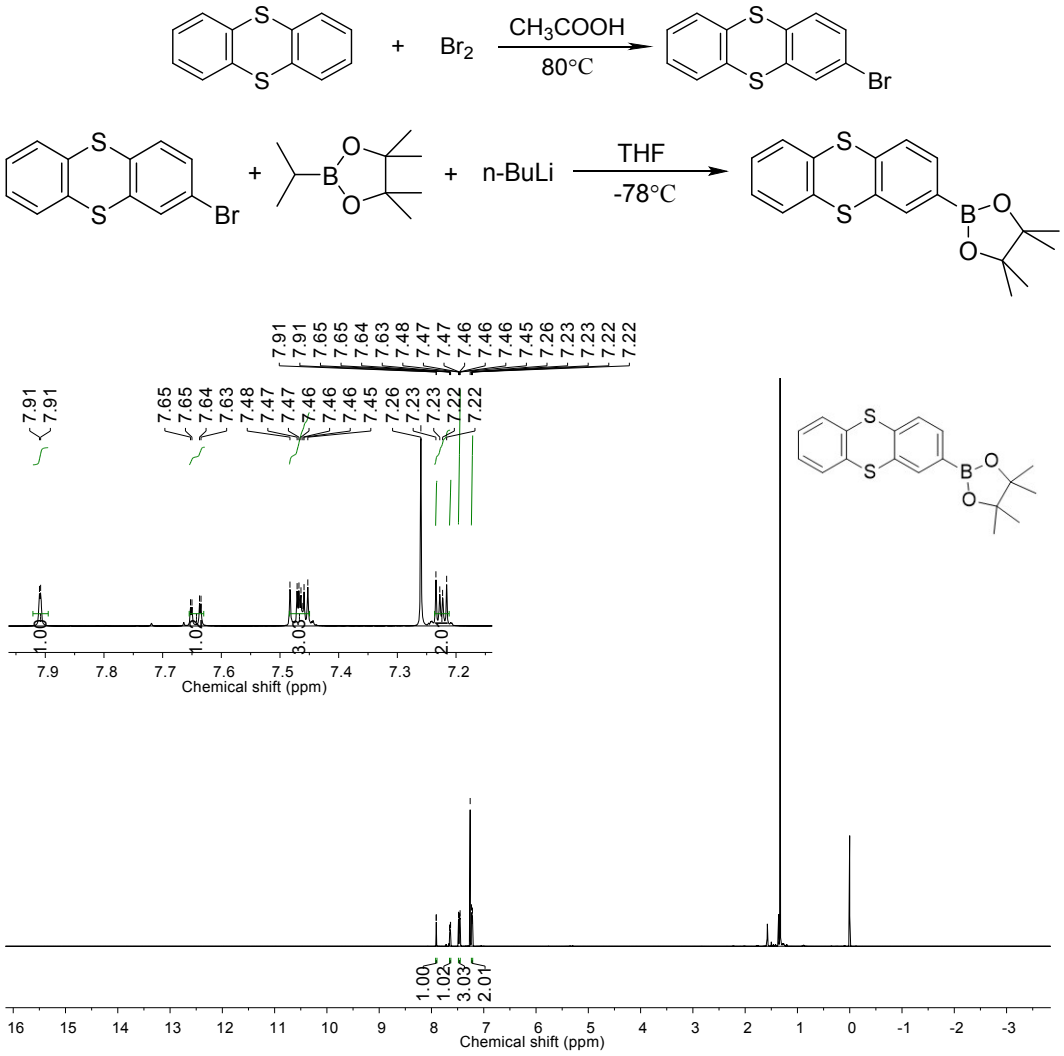

(a) ^{1}H NMR spectrum of TE-BPin in d-$CDCl_3$ solvent.

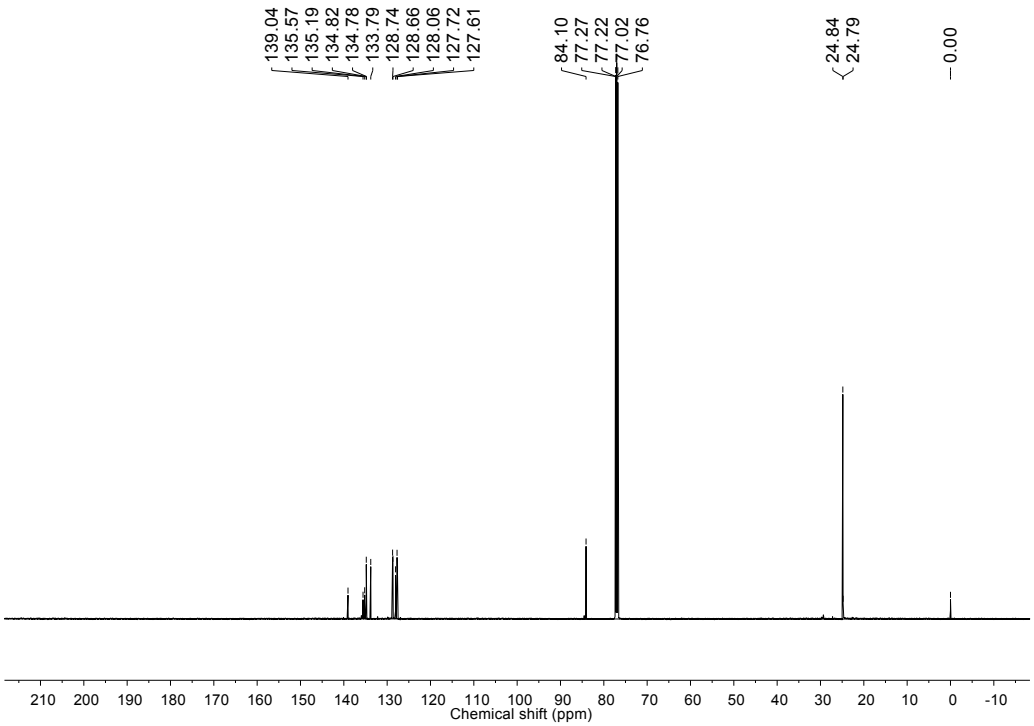

(b) ^{13}C NMR spectrum of TE-BPin in *d*-$CDCl_3$ solvent.

PXT. ^{1}H NMR (500 MHz, $CDCl_3$) δ 7.15 – 7.08 (m, 1H), 7.03 – 6.98 (m, 1H). ^{13}C NMR (126 MHz, $CDCl_3$) δ 152.17, 127.70, 126.77, 124.51, 120.13, 117.80, 77.24, 77.01, 76.76, 0.00. Calcd ($C_{12}H_8OS$): 200.26, APCI-MS (mass m/z); found: 200.4 ((M+1)+).

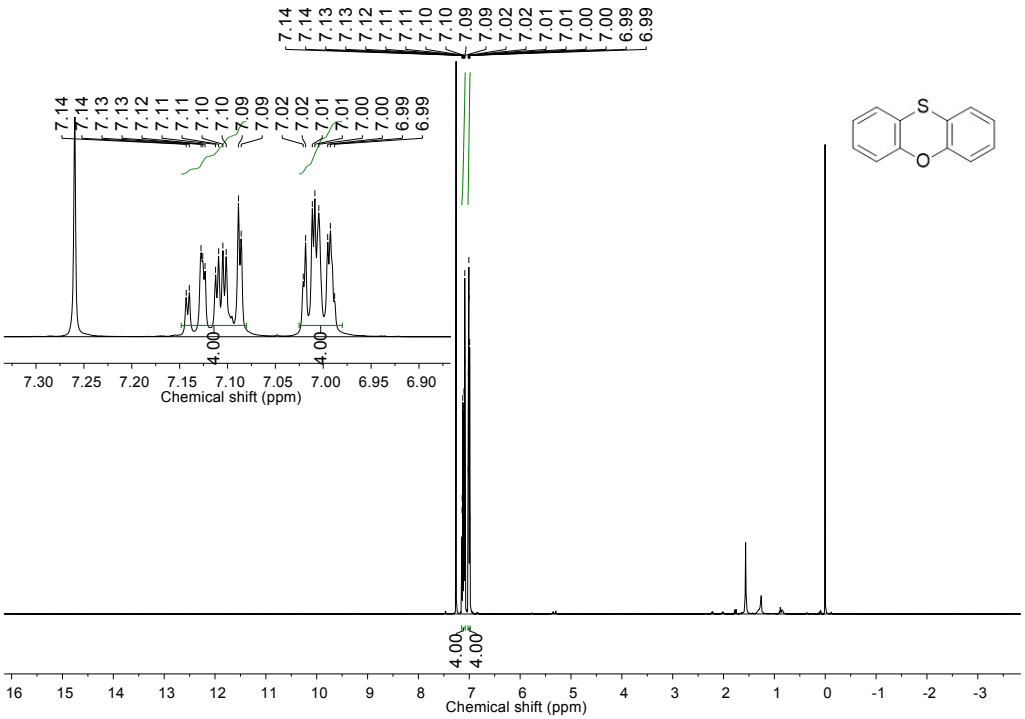

(a) ^{1}H NMR spectrum of PXT in *d*-$CDCl_3$ solvent.

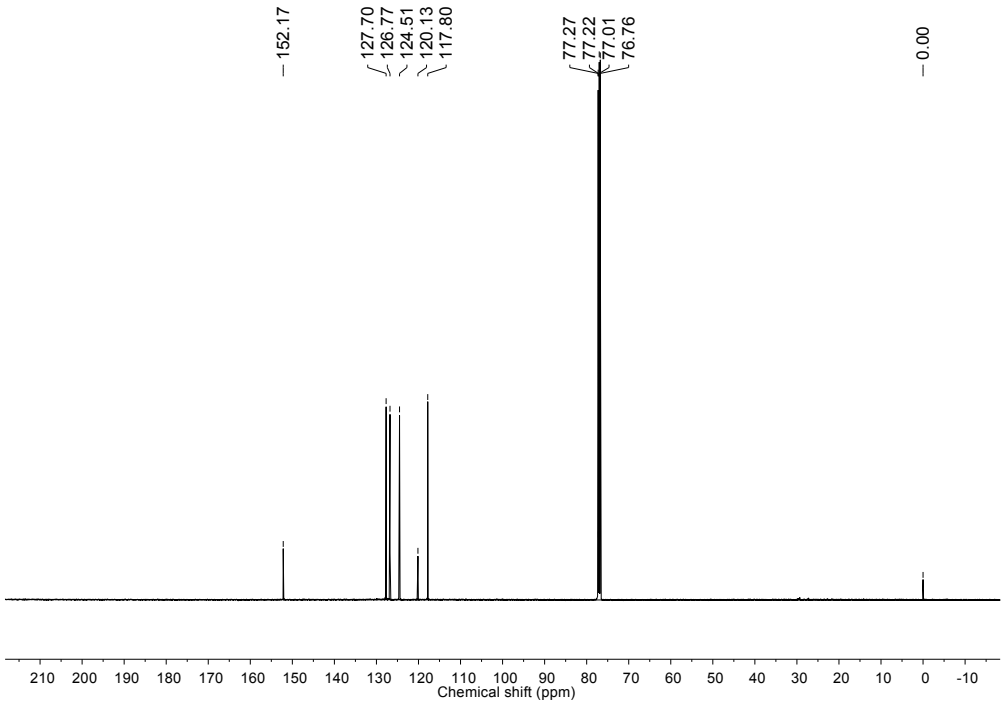

(b) ^{13}C NMR spectrum of PXT in *d*-$CDCl_3$ solvent.

PXT-BPin. 2-Mercaptophenol and 1,4-dibromo-2-nitrobenzene was obtained from commercial sources. In a 250 mL flask, 16 g potassium *tert*-butoxide was added, and then solved with dry DMF (150 mL). After stirring 10 minutes, 2-mercaptophenol (3.2 g) was added into the mixture. After stirring an hour at room temperature, 1,4-dibromo-2-nitrobenzene (7.2 g) was added into the mixture. And then after stirring 3 hours at room temperature, the mixture was heated up to 150 ℃ and reacted 12 hours at this temperature. When the reaction was finished, the resultant was treated by extraction with dichloromethane, drying with anhydrous magnesium sulfate, solvent evaporation and purified by chromatographic column.

The product derived from the step forward was added into a 250 mL flask and cooled to -78℃, and then n-butyllithium (8.2 mL, 2.4 M) was added into the solution dropwise. After an hour, isopropoxyboronic acid pinacol ester (6.0 g) was added into the solution dropwise, and then the reaction was kept for 12 hours after stopping cooling. The resultant was solved by extraction with dichloromethane, drying with anhydrous magnesium sulfate, solvent evaporation and purified by chromatographic column. ^1H NMR (500 MHz, $CDCl_3$) δ 7.41 (dt, J = 4.4, 1.1 Hz, 2H), 7.13 – 7.06 (m, 3H), 6.98 (ddd, J = 16.7, 7.8, 1.3 Hz, 2H). ^{13}C NMR (126 MHz, $CDCl_3$) δ 13.85, 13.23, -7.64, -10.52, -11.61, -12.11, -13.90, -14.40, -14.84, -18.57, -20.48, -54.32, -61.07, -61.30, -61.55, -113.46, -138.31. Calcd ($C_{18}H_9BO_3S$): 326.22, APCI-MS (mass m/z); found: 326.3 ((M+1)+).

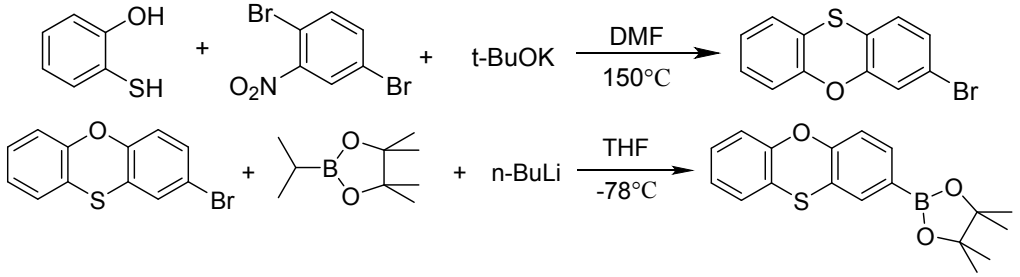

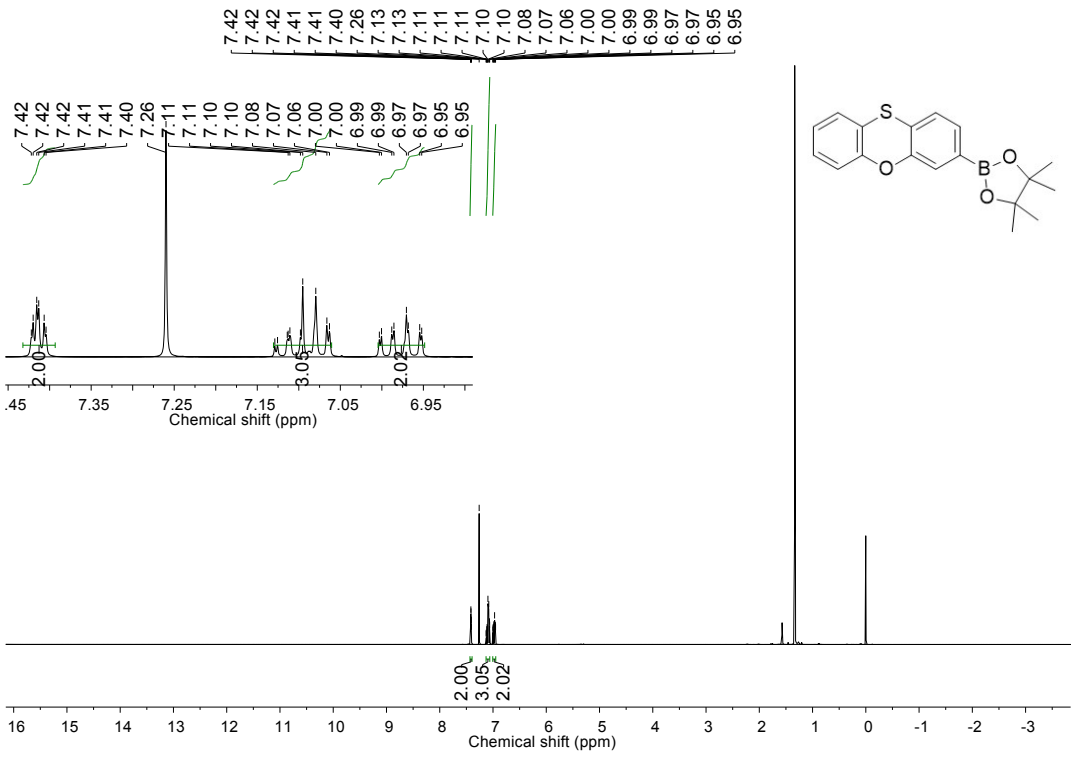

(a) ^{1}H NMR spectrum of PXT-BPin in *d*-$CDCl_3$ solvent.

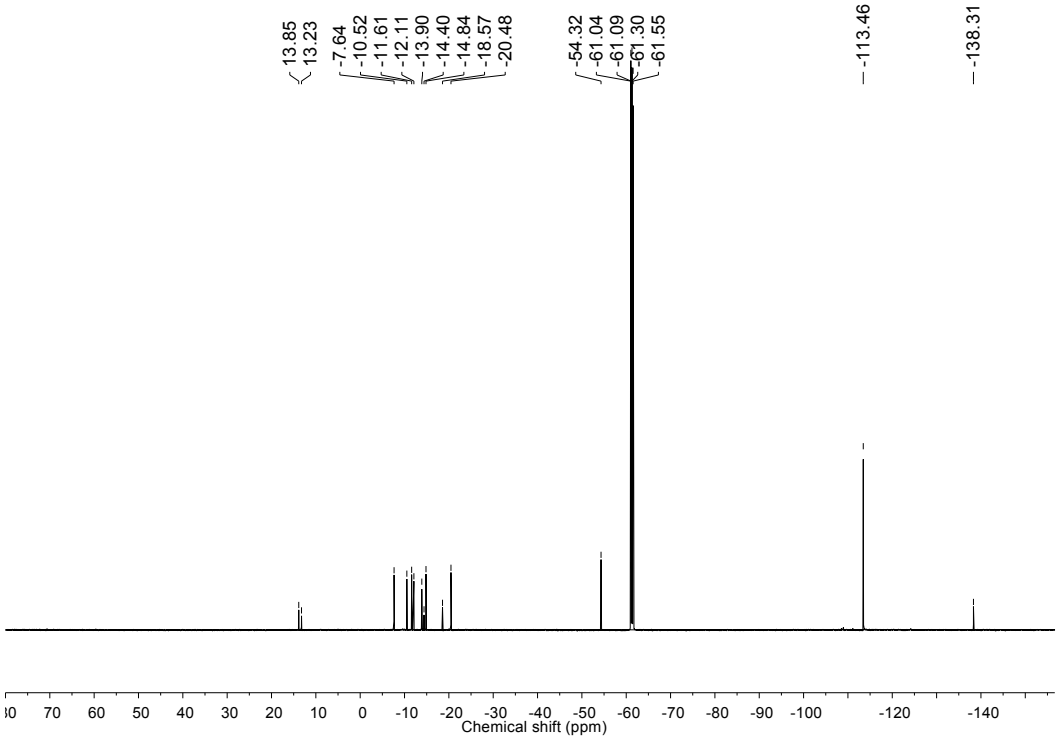

(b) ^{13}C NMR spectrum of PXT-BPin in *d*-$CDCl_3$ solvent.

i-PXT-BPin. 2-Mercaptophenol and 2,4-dibromo-1-nitrobenzene was obtained from commercial sources. In a 250 mL flask, 16 g potassium *tert*-butoxide was added, and then solved with dry DMF (150 mL). After stirring 10 minutes, 2-mercaptophenol (4.5 g) was added into the mixture. After stirring an hour at room temperature, 2,4-dibromo-1-nitrobenzene (10 g) was added into the mixture. And then after stirring 3 hours at room temperature, the mixture was

heated up to 150 ℃ and reacted 12 hours at this temperature. When the reaction was finished, the resultant was treated by extraction with dichloromethane, drying with anhydrous magnesium sulfate, solvent evaporation and purified by chromatographic column.

The product derived from the step forward was added into a 250 mL flask and cooled to -78 ℃, and then n-butyllithium (6.3 mL, 1.6 M) was added into the solution dropwise. After an hour, isopropoxyboronic acid pinacol ester (3.4 g) was added into the solution dropwise, and then the reaction was kept for 12 hours after stopping cooling. The resultant was solved by extraction with dichloromethane, drying with anhydrous magnesium sulfate, solvent evaporation and purified by chromatographic column. ^{1}H NMR (500 MHz, $CDCl_3$) δ 7.58 – 7.51 (m, 1H), 7.13 – 7.05 (m, 1H), 7.01 – 6.95 (m, 2H). ^{13}C NMR (126 MHz, $CDCl_3$) δ 154.35, 151.66, 134.52, 133.31, 127.58, 126.77, 124.59, 119.96, 119.28, 117.75, 117.18, 83.96, 77.25, 77.02, 76.76, 24.84, 0.00. Calcd ($C_{18}H_9BO_3S$): 326.22, APCI-MS (mass m/z); found: 326.4 ((M+1)+).

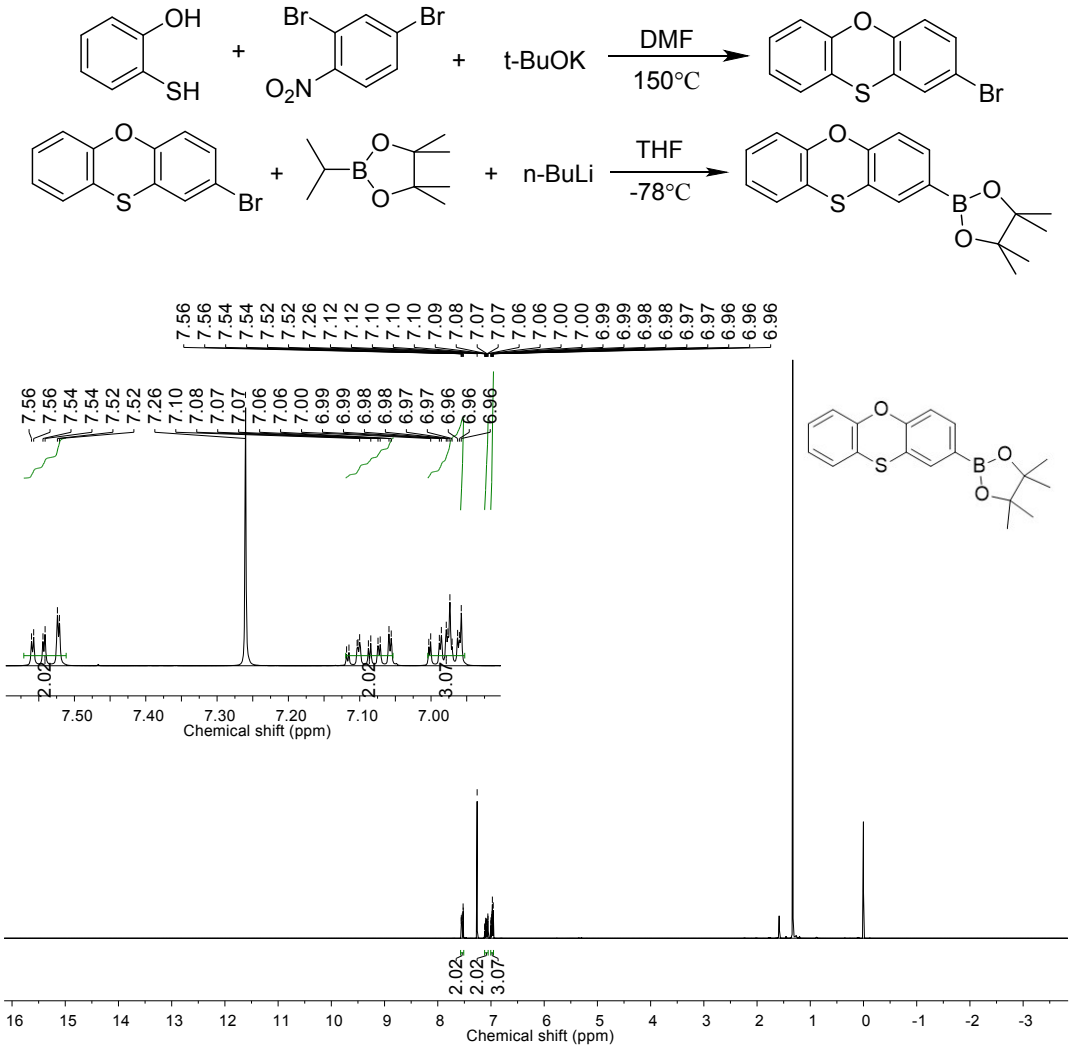

(a) ^{1}H NMR spectrum of i- PXT-BPin in *d*-$CDCl_3$ solvent.

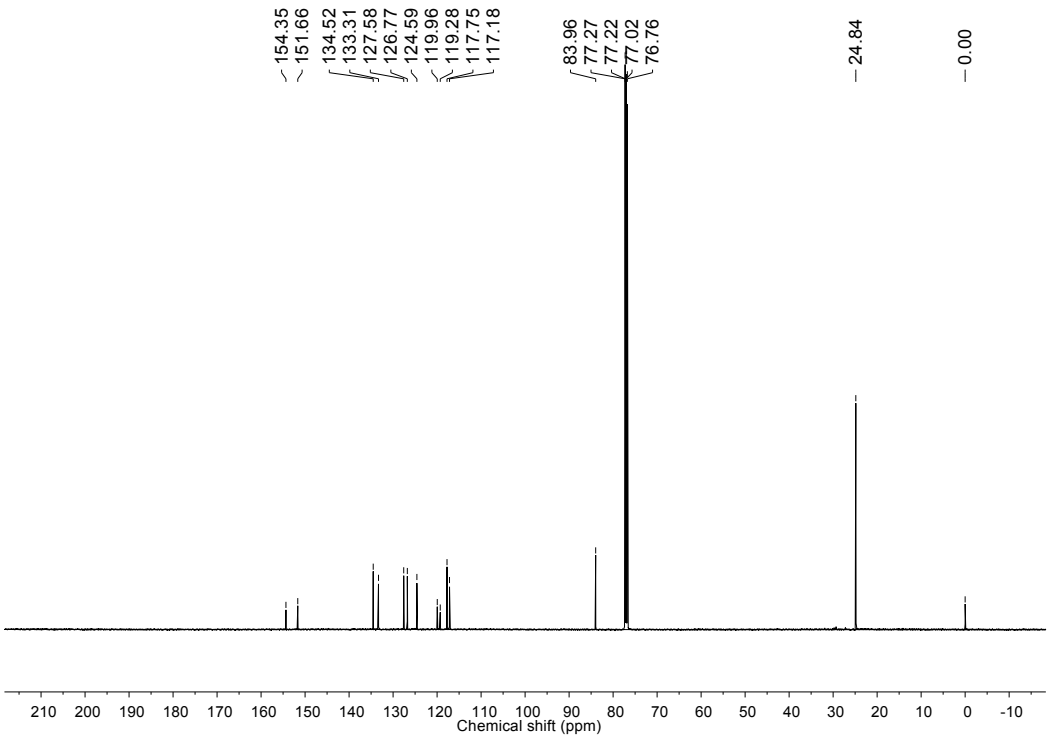

(a) ^{13}C NMR spectrum of i- PXT-BPin in *d*-$CDCl_3$ solvent.

3. Thermal Properties

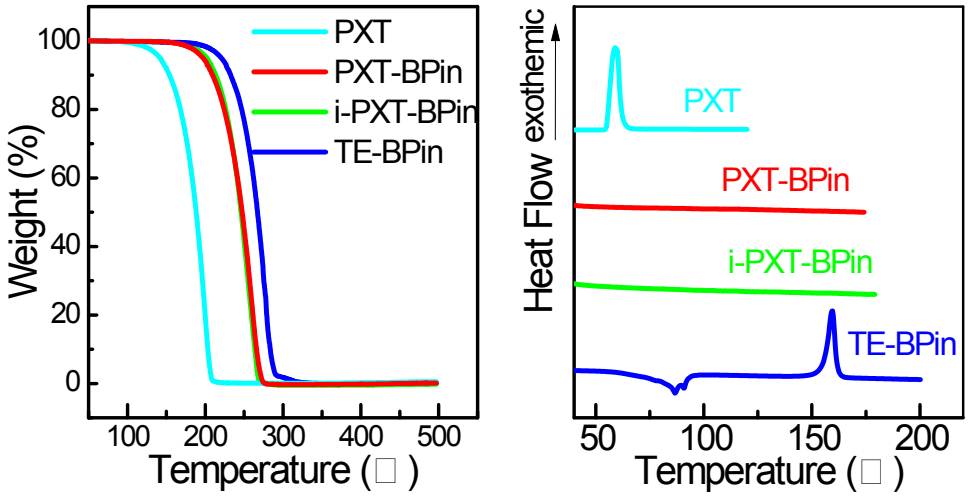

Fig. S1 (a) TGA curves and (b) DSC curves of PXT, PXT-BPin, i-PXT-BPin and TE-BPin.

4. Photophysical Characterization

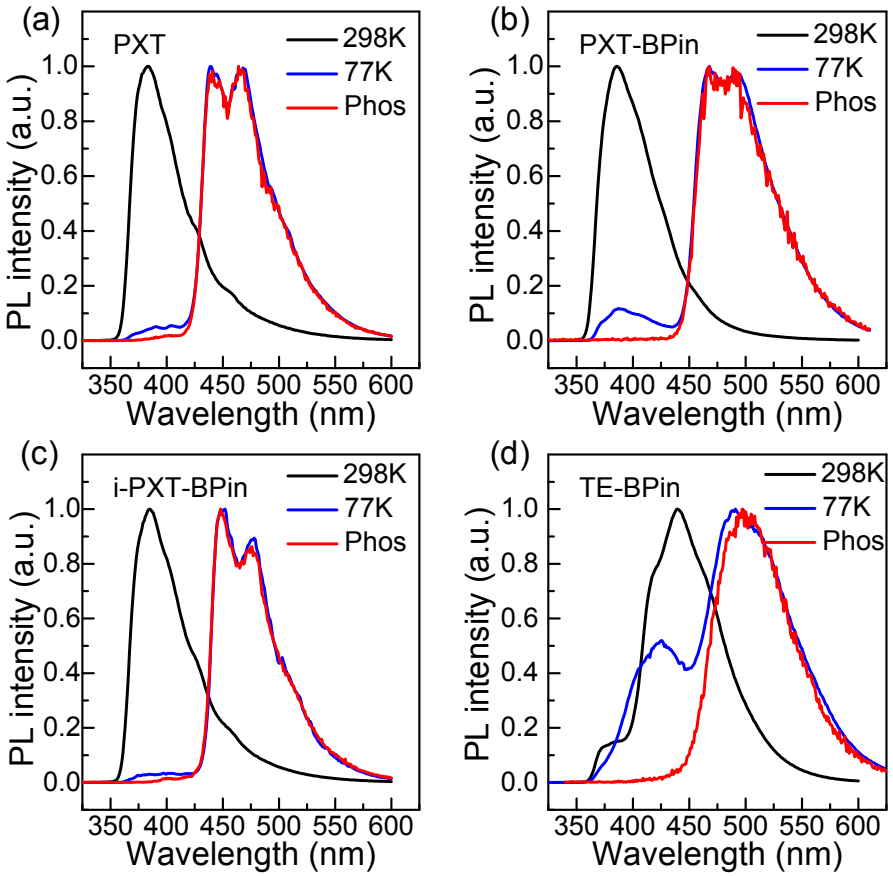

Fig. S2 Photoluminescence (PL) spectra of (a) PXT, (b) PXT-BPin, (c) i-PXT-BPin and (d) TE-BPin in n-hexane measured under N_2. (1×10^{-4} M) (Phosphorescence spectra were recorded after 40 ms delay).

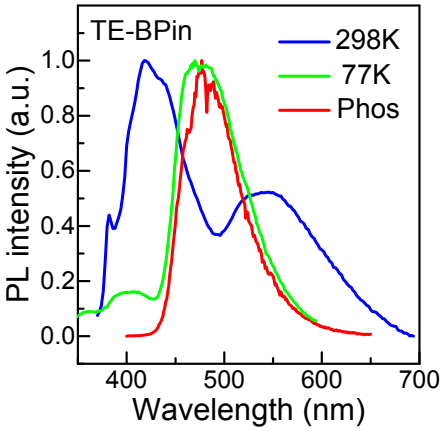

Fig. S3 Steady-state PL (blue and green lines for fluorescence measured at 298K and 77K, respectively) and phosphorescence spectra (red lines for phosphorescence spectra detected at 77 K with 40ms time delay) of (a) PXT, (b) PXT-BPin and (c) i-PXT-BPin in crystal.

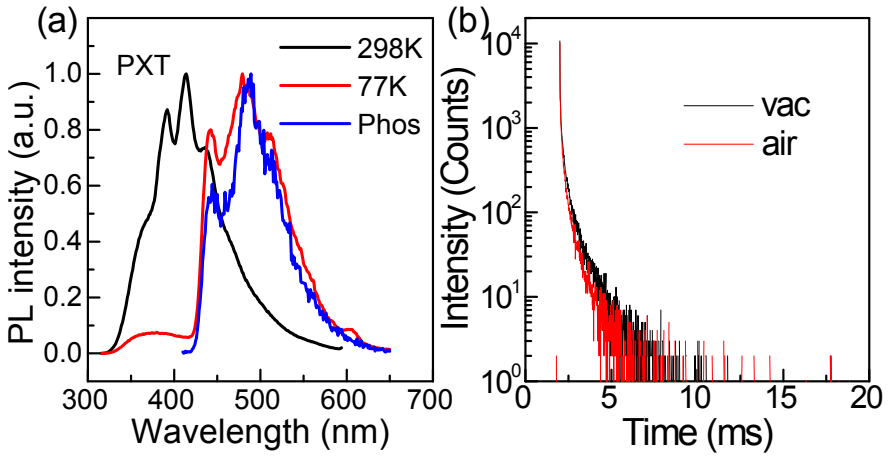

Fig. S4 (a) PL spectra and (b) phosphorescence transient decay spectra of PXT powder (Insert: fluorescence transient decay spectra at 370 nm).

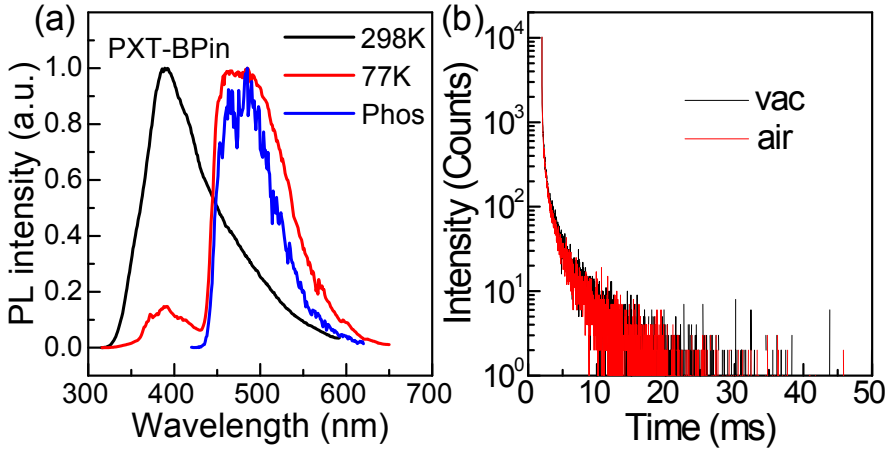

Fig. S5 (a) PL spectra and (b) phosphorescence transient decay spectra of PXT-BPin powder (Insert: fluorescence transient decay spectra at 391 nm).

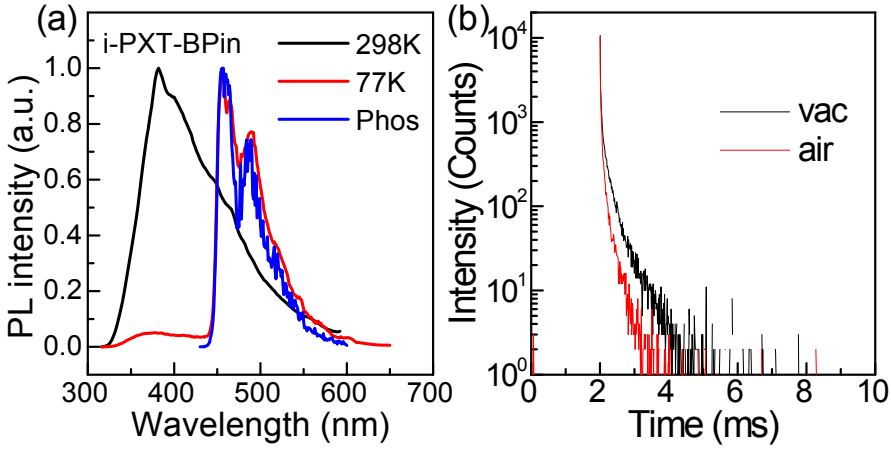

Fig. S6 (a) PL spectra and (b) phosphorescence transient decay spectra of i-PXT-BPin powder (Insert: fluorescence transient decay spectra at 395 nm).

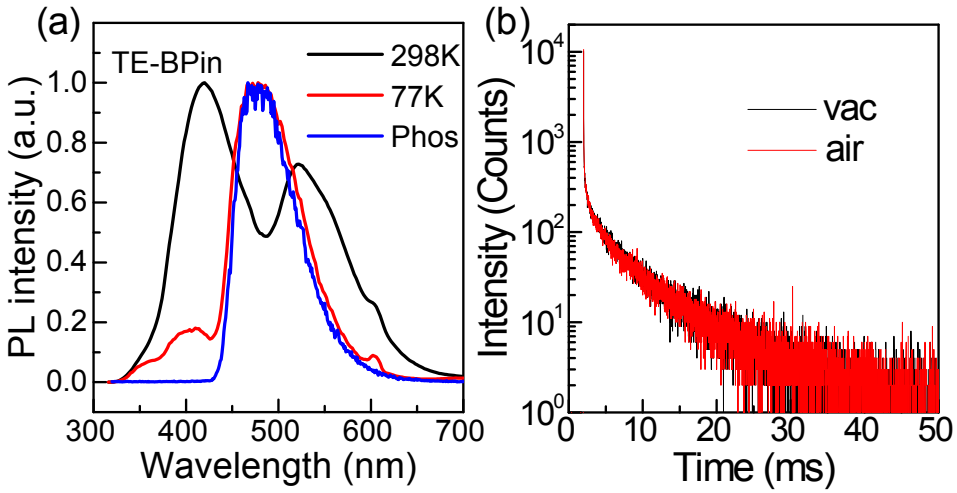

Fig. S7 (a) PL spectra and (b) phosphorescence transient decay spectra of TE-BPin powder (Insert: fluorescence transient decay spectra at 420 nm).

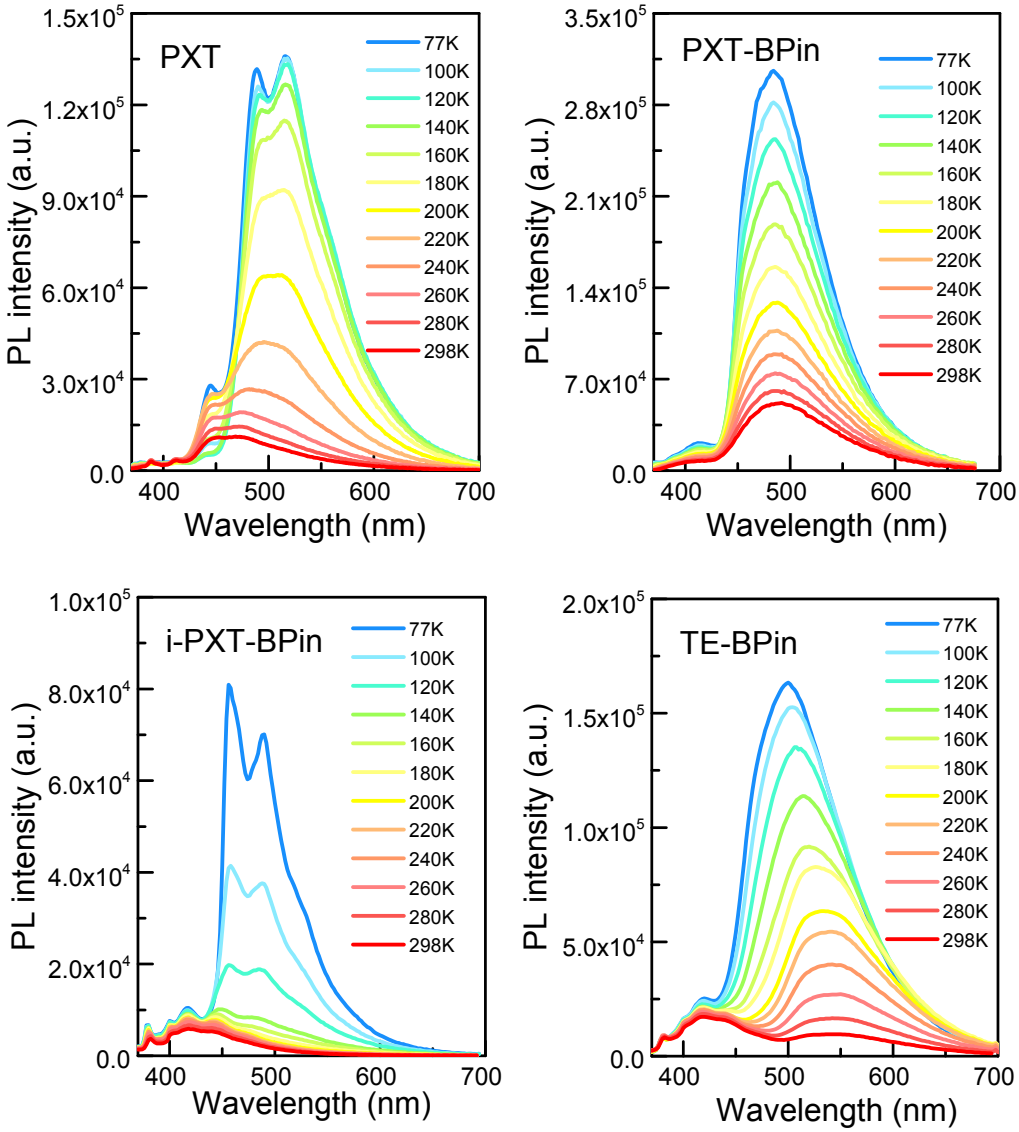

Fig. S8 Temperature-dependent PL spectra of (a) PXT, (b) PXT-BPin, (c) i-PXT-BPin and (d) TE-BPin in crystal states.

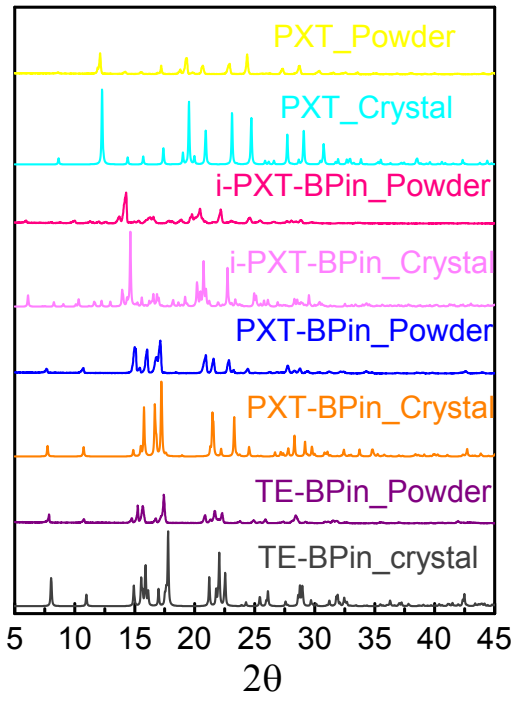

Fig. S9 XRD patterns of i-PXT-BPin, PXT and TE-BPin in powder and crystal states, respectively.

5. Theoretical Calculation

All of the simulations were performed using the Gaussian 09_B01 program package.[1] The ground state geometries of all monomers were optimized using B3LYP functional with 6-31G* basis set in vacuum, and the vibrational frequencies were further calculated based on the optimized structures to confirm that the local minima were found.[2] For monomers, the excitation energies of the singlet excited states (S_1) and n-th triplet excited states (T_n) were calculated with TD-DFT method based on the optimized ground state geometries using M06-2X functional with 6-311G** basis set.[3] For stacking structures of crystals, the corresponding excitation energies were calculated using the same method based on the geometries selected form single crystals directly.

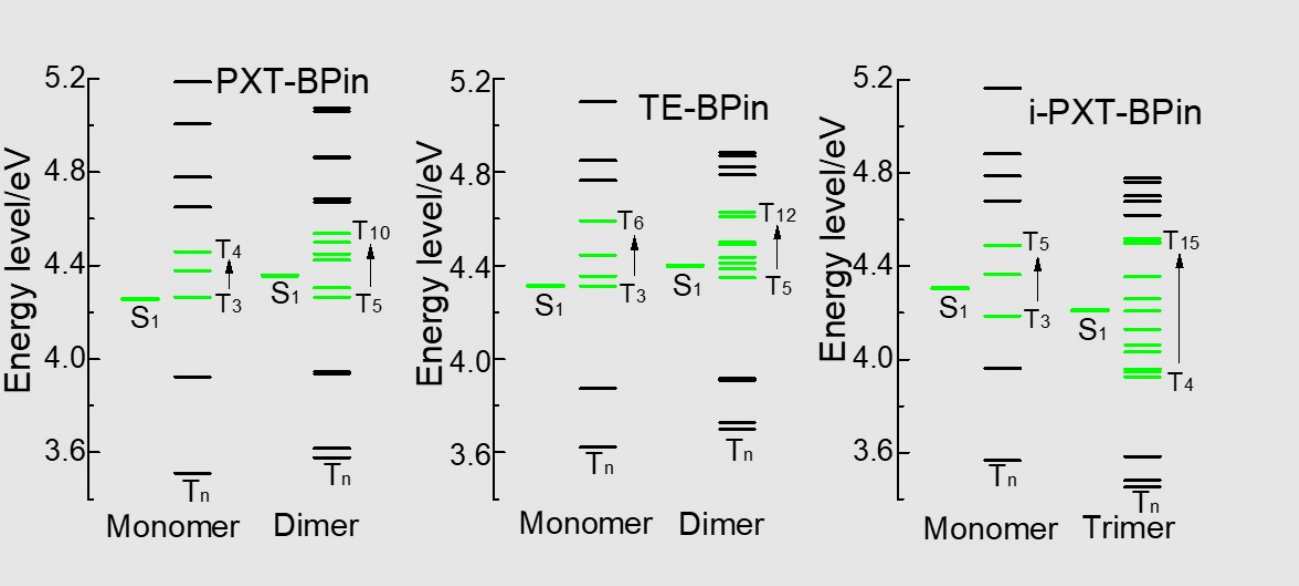

Fig. S10 Energy levels of monomers and corresponding packing units of PXT-BPin, TE-BPin and i-PXT-BPin (The energy levels marked by the green solid lines represent the excited states with the same configurations with S_1).

Table S2. Calculated singlet and triplet excited states transition configurations of PXT monomer by TD-DFT method (Only the ratio of transition configurations exceed 3% are given).

Energy level	Transition configuration (%)
S_1	H→L (87.29); H→L+4 (7.58);
T_1	H-3→L+1 (5.10); H-2→L+3 (8.18); H-1→L+2 (5.80); H→L (77.66)
T_2	H-3→L (4.32); H-3→L+2 (8.70); H-2→L (15.54); H-1→L+1 (10.36); H→L+1 (34.29); H→L+3 (21.43);
T_3	H-2→L+2 (16.71); H-1→L+1 (10.63); H-1→L+3 (3.93); H→L+1 (50.35); H→L+3 (13.94)
T_4	H-2→L+1 (15.46); H-1→L+2 (6.80); H→L+2 (68.87)
T_5	H-3→L+1 (30.75); H-1→L (3.47); H-1→L+2 (36.05); H→L (7.87); H→L+2 (6.37); H→L+4 (8.48)
T_6	H-3→L (2.09); H-3→L+2 (17.17); H-2→L (12.79); H-1→L+1 (40.53); H→L+3 (24.53)
T_7	H-2→L+1 (3.32); H-2→L+3 (3.19); H-1→L (26.06); H→L+4 (51.54);
T_8	H-3→L+3 (15.92); H-1→L (45.96); H-1→L+2 (6.99); H→L+2 (5.16); H→L+4 (17.63)
T_9	H-3→L (43.26); H-3→L+2 (5.01); H-1→L+3 (38.67); H→L+3 (5.92)
T_{10}	H-3→L (7.82); H-2→L (27.20); H→L+3 (14.64); H→L+5 (18.00); H→L+7 (7.65); H→L+8 (7.74)
T_{11}	H-4→L+1 (7.75); H-3→L+2 (4.86); H-2→L (13.49); H-2→L+2 (9.24); H→L+1 (4.58); H→L+3 (5.34); H→L+5 (23.71); H→L+7 (10.85); H→L+8 (7.96)
T_{12}	H-4→L (11.91); H-4→L+2 (3.89); H-3→L+1 (9.31); H-3→L+3 (3.42); H-2→L+1 (38.61); H-2→L+3 (5.46); H→L (5.75); H→L+2 (8.44); H→L+4 (3.39)
T_{13}	H-4→L+1 (8.22); H-3→L+2 (8.60); H-2→L (5.49); H-2→L+2 (42.29); H→L+1 (4.30); H→L+3 (10.47); H→L+5 (6.25)
T_{14}	H-4→L (12.35); H-4→L+2 (7.38); H-3→L+3 (5.32); H-2→L+1 (11.57); H-2→L+3 (38.31); H→L+2 (8.13)
T_{15}	H-3→L+3 (6.52); H-2→L+1 (5.31); H-2→L+3 (3.47); H-1→L (8.21); H-1→L+4 (53.70); H→L+4 (6.34)
T_{16}	H-3→L (29.74); H-3→L+2 (3.27); H-2→L (11.49); H-1→L+1 (15.25); H-1→L+3 (27.28)
T_{17}	H-3→L+1 (33.41); H-2→L+1 (11.26); H-1→L+2 (28.53); H-1→L+4 (8.05)
T_{18}	H-3→L+2 (31.35); H-2→L+2 (12.16); H-1→L+1 (17.25); H-1→L+3 (16.41); H-1→L+5 (4.00); H→L+5 (3.03)
T_{19}	H-5→L (29.31); H-4→L (3.32); H-4→L+4 (8.18); H-3→L+3 (5.72); H-1→L+2 (3.03)
T_{20}	H-3→L+4 (8.14); H-2→L+4 (21.98); H-1→L+5 (5.80); H→L+5 (14.55); H→L+7 (22.68); H→L+8 (3.99)

Table S3. Calculated singlet and triplet excited states transition configurations of PXT tetramer by TD-DFT method (Only the ratio of transition configurations exceed 3% are given).

Energy level	Transition configuration (%)
S_1	H-3→L (7.96); H-2→L+2 (3.47); H-1→L (13.58); H-1→L+2 (20.25); H-1→L+3 (13.67); H-1→L+4 (9.38)
T_1	H-9→L+13 (5.01); H-5→L+10 (3.88); H-1→L (9.18); H-1→L+2 (23.91); H-1→L+3 (13.91); H-1→L+4 (9.33); H-1→L+7 (3.22)
T_2	H-8→L+15 (6.82); H-4→L+11 (4.48); H-3→L (4.43); H→L+2 (5.88); H→L+4 (7.63); H→L+6 (50.28)
T_3	H-11→L+14 (4.79); H-6→L+9 (3.80); H-3→L (4.87); H-2→L+2 (7.93); H-2→L+3 (39.26); H-2→L+4 (9.12); H-1→L+3 (3.05); H→L+6 (3.19)
T_4	H-14→L+12 (5.01); H-7→L+7 (3.05); H-3→L (51.82); H-3→L+1 (5.51); H-2→L+3 (3.90)
T_5	H-12→L+10 (3.02); H-9→L+2 (4.84); H-9→L+3 (3.15); H-5→L+2 (3.43); H-1→L+2 (9.13); H-1→L+4 (14.20); H-1→L+8 (3.86); H-1→L+13 (13.65); H-1→L+14 (3.93)
T_6	H-10→L+11 (6.30); H-8→L+6 (11.90); H-4→L+8 (4.75); H→L+4 (7.79); H→L+6 (3.25); H→L+8 (18.07); H→L+11 (3.43); H→L+15 (20.02)
T_7	H-13→L+9 (4.76); H-11→L+3 (8.60); H-6→L+5 (5.95); H-2→L+5 (23.64); H-2→L+13 (4.04); H-2→L+14 (14.04)
T_8	H-15→L+7 (4.78); H-14→L (12.65); H-7→L+1 (5.63); H-3→L+1 (28.39); H-3→L+12 (20.02)
T_9	H-11→L+9 (8.63); H-6→L+5 (6.07); H-2→L+5 (36.05); H-2→L+9 (3.71); H-2→L+14 (7.69); H-1→L+5 (4.22)
T_{10}	H-9→L+10 (7.50); H-1→L+2 (7.67); H-1→L+4 (12.71); H-1→L+6 (4.74); H-1→L+8 (6.04); H-1→L+13 (7.87); H→L+8 (4.76); H→L+15 (3.18)
T_{11}	H-8→L+11 (8.41); H-4→L+8 (4.13); H-1→L+4 (4.84); H→L+8 (27.19); H→L+9 (3.02); H→L+11 (3.44); H→L+15 (8.72)
T_{12}	H-14→L+7 (7.27); H-7→L+1 (5.03); H-3→L+1 (43.28); H-3→L+5 (3.35); H-3→L+12 (11.63)
T_{13}	H-9→L+4 (6.08); H-5→L+10 (3.20); H-2→L+10 (5.32); H-1→L+8 (4.22); H-1→L+9 (6.80); H-1→L+10 (43.20)
T_{14}	H-14→L+1 (10.38); H-7→L+7 (4.57); H-3→L+3 (5.34); H-3→L+7 (47.80); H-3→L+8 (3.19)
T_{15}	H-11→L+5 (9.03); H-6→L+9 (3.80); H-2→L+8 (3.70); H-2→L+9 (42.53); H-2→L+10 (8.80); H-2→L+14 (3.29); H-1→L+9 (4.91)
T_{16}	H-8→L+8 (5.71); H-8→L+15 (3.25); H-4→L+11 (5.29); H→L+10 (4.53); H→L+11 (53.09); H→L+15 (4.57)
T_{17}	H-12→L+2 (5.86); H-12→L+4 (5.28); H-5→L+8 (3.93); H-5→L+10 (24.92); H-1→L+10 (3.32)
T_{18}	H-15→L (4.17); H-15→L+1 (21.47); H-12→L+1 (3.19); H-7→L (3.91); H-7→L+3 (3.47); H-7→L+7 (21.93); H-3→L (6.74); H-3→L+7 (5.27); H-3→L+16 (3.14)
T_{19}	H-10→L+4 (4.51); H-10→L+8 (15.70); H-4→L+11 (32.34); H→L+6 (6.01); H→L+11 (4.28); H→L+19 (3.06)
T_{20}	H-10→L+4 (4.51); H-10→L+8 (15.70); H-4→L+11 (32.34); H→L+6 (6.01); H→L+11 (4.28); H→L+19 (3.06)

Table S4. Calculated singlet and triplet excited states transition configurations of PXT-BPin monomer by TD-DFT method (Only the ratio of transition configurations exceed 3% are given).

Energy level	Transition configuration (%)
S_1	H→L (82.97); H→L+1 (6.31); H→L+4 (3.63)
T_1	H-2→L (6.05); H-2→L+3 (3.67); H→L (75.25)
T_2	H-3→L+1 (3.28); H-3→L+2 (4.55); H-2→L (9.06); H-2→L+1 (3.48); H-1→L+1 (4.02); H→L+1 (44.36); H→L+3 (12.98)
T_3	H-3→L (3.66); H-3→L+2 (3.48); H-2→L+2 (13.61); H-1→L (12.08); H-1→L+1 (9.40); H-1→L+3 (6.00); H→L (4.58); H→L+1(28.58); H→L+3 (13.10)
T_4	H-3→L (6.20); H-2→L (4.37); H-2→L+1 (7.10); H-1→L (10.81); H-1→L+2 (15.37); H→L+1 (5.75); H→L+2 (37.37)
T_5	H-3→L (9.04); H-3→L+1 (4.06); H-2→L+1 (3.89); H-2→L+3 (3.29); H-1→L (31.99); H→L+2 (22.95); H→L+3 (13.59)
T_6	H-3→L+1 (15.90); H-3→L+2 (8.02); H-2→L (4.15); H-1→L+1 (11.60); H-1→L+2 (19.28); H→L+2 (7.28); H→L+3 (8.88); H→L+4 (10.76)
T_7	H-3→L+2 (3.02); H-2→L+1 (5.13); H-1→L (3.72); H-1→L+1 (22.92); H→L+3 (5.61); H→L+4 (42.19)
T_8	H-3→L+3 (12.56); H-1→L (9.66); H-1→L+1 (9.19); H-1→L+2 (12.76); H-1→L+3 (6.20); H→L+2 (6.13); H→L+3 (7.86); H→L+4 (21.05)
T_9	H-3→L (17.86); H-3→L+1 (10.30); H-3→L+2 (13.43): H-3→L+3 (3.05); H-1→L+2 (3.90); H-1→L+3 (31.01); H→L+3 (5.76)
T_{10}	H-5→L (9.04); H-3→L (7.83); H-2→L (46.62); H→L (9.08); H→L+3 (8.96)
T_{11}	H-5→L (4.13); H-3→L+1 (3.36); H-2→L+1 (15.02); H→L+3 (3.76); H→L+6 (25.15); H→L+8 (15.98)
T_{12}	H-5→L+1 (10.13); H-3→L+1 (3.28); H-2→L+1 (24.22); H-2→L+2 (3.86); H-2→L+3 (3.29); H→L+1 (5.92); H→L+3 (3.58); H→L+6 (13.54); H→L+8 (8.27)
T_{13}	H-7→L (3.71); H-4→L (67.43); H-4→L+3 (3.56); H-4→L+13 (5.22)
T_{14}	H-5→L (5.67); H-5→L+2 (5.72); H-3→L+2 (4.68); H-2→L+2 (37.75); H-2→L+3 (7.12); H→L+2 (6.34); H→L+3 (6.44); H→L+6 (4.44)
T_{15}	H-8→L (3.12); H-7→L (6.84); H-4→L (3.28); H-3→L (14.58); H-3→L+2 (3.56); H-2→L (3.49); H-2→L+3 (18.72); H-1→L (8.67)
T_{16}	H-8→L (3.44); H-7→L (9.50); H-5→L+1 (3.91); H-5→L+2 (3.41); H-3→L (12.66); H-3→L+3 (3.35); H-2→L (4.70); H-2→L+1 (6.76); H-2→L+2 (5.97); H-2→L+3 (16.51); H-1→L (4.96)
T_{17}	H-8→L (7.92); H-7→L (30.67); H-5→L (16.70); H-3→L (7.75); H-2→L (5.98); H-1→L (6.02); H-1→L+4 (3.37)
T_{18}	H-7→L (2.19); H-3→L+1 (7.54); H-3→L+3 (7.82); H-2→L+1 (7.27); H-1→L+1 (10.74); H-1→L+3 (11.92); H-1→L+4 (33.44); H→L+4 (4.66)
T_{19}	H-3→L+1 (26.16); H-3→L+2 (3.32); H-2→L+1 (7.66); H-1→L+1 (7.72); H-1→L+2 (18.62); H-1→L+4 (19.98)
T_{20}	H-5→L (2.69); H-3→L+2 (28.38); H-2→L+2 (8.97); H-1→L+1 (5.20); H-1→L+2 (3.20); H-1→L+3 (19.09); H-1→L+4 (8.20)

Table S5. Calculated singlet and triplet excited states transition configurations of PXT-BPin dimer by TD-DFT method (Only the ratio of transition configurations exceed 3% are given).

Energy level	Transition configuration (%)
S_1	H-1→L (80.18); H-1→L+2 (7.67); H-1→L+8 (3.39)
T_1	H-7→L (2.15); H-6→L (8.13); H-6→L+5 (3.55); H-1→L (73.16)
T_2	H-4→L+1 (6.68); H-4→L+7 (3.67); H→L+1 (73.00)
T_3	H-7→L+2 (2.94); H-7→L+4 (4.81); H-6→L (7.17); H-6→L+2 (5.25); H-6→L+5 (4.20); H-3→L+2 (3.60); H-1→L+2 (41.41); H-1→L+5 (16.72)
T_4	H-5→L+3 (3.90); H-5→L+6 (4.45); H-4→L+1 (9.42); H-4→L+3 (5.46); H-2→L+3 (4.11); H→L+3 (43.01); H→L+6 (6.21); H→L+7 (11.11)
T_5	H-7→L+4 (4.43); H-6→L+4 (13.63); H-3→L (5.16); H-3→L+2 (8.71); H-3→L+5 (6.16); H-1→L (6.41); H-1→L+2 (31.28); H-1→L+5 (18.89)
T_6	H-5→L+6 (4.74); H-4→L+6 (13.43); H-2→L+1 (4.51); H-2→L+3 (7.58); H-2→L+7 (6.41); H→L+1 (4.17); H→L+3 (34.29); H→L+6 (3.98); H→L+7 (16.56)
T_7	H-6→L+2 (10.12); H-6→L+5 (3.86); H-3→L+4 (13.39); H-1→L+2 (3.95); H-1→L+4 (52.44)
T_8	H-4→L+3 (9.42); H-4→L+7 (4.61); H-2→L+1 (3.69); H-2→L+6 (14.58); H→L+1 (3.36); H→L+6 (43.91); H→L+7 (3.56)
T_9	H-7→L (18.64); H-7→L+2 (4.90); H-3→L (40.56); H-3→L+4 (3.79); H-1→L+4 (11.61); H-1→L+5 (8.82)
T_{10}	H-5→L+1 (12.88); H-5→L+3 (5.86); H-2→L+1 (41.92); H-2→L+6 (4.76); H→L+6 (10.11); H→L+7 (12.93)
T_{11}	H-7→L+2 (17.69); H-7→L+4 (9.99); H-6→L (3.38); H-3→L+2 (18.62); H-3→L+4 (17.19); H-1→L+4 (5.53); H-1→L+5 (12.36); H-1→L+8 (3.08)
T_{12}	H-5→L+3 (23.59); H-5→L+6 (8.76); H-4→L+1 (3.64); H-2→L+1 (3.16); H-2→L+3 (19.46); H-2→L+6 (10.10); H→L+6 (7.69); H→L+7 (9.38); H→L+10 (4.99)
T_{13}	H-7→L+5 (6.61); H-3→L (10.67); H-3→L+2 (22.42); H-3→L+4 (4.42); H-1→L+5 (4.13); H-1→L+8 (27.93); H-1→L+9 (3.70)
T_{14}	H-5→L+7 (5.55); H-4→L+3 (3.56); H-2→L+1 (9.47); H-2→L+3 (16.99); H-2→L+6 (4.33); H→L+7 (5.37); H→L+10 (38.12)
T_{15}	H-7→L (4.77); H-7→L+2 (5.70); H-7→L+5 (6.13); H-3→L (5.76); H-3→L+2 (3.11); H-3→L+4 (6.60); H-3→L+5 (11.88); H-1→L+4 (3.03); H-1→L+5 (5.11); H-1→L+8 (29.29); H-1→L+9 (3.90)
T_{16}	H-5→L+1 (3.26); H-5→L+7 (9.26); H-2→L+1 (9.14); H-2→L+3 (3.01); H-2→L+6 (7.36); H-2→L+7 (15.63); H→L+6 (3.21); H→L+7 (7.30); H→L+10 (27.54)
T_{17}	H-7→L (11.48); H-7→L+2 (8.57); H-7→L+4 (9.76); H-7→L+5 (8.20); H-3→L+2 (4.71); H-3→L+4 (5.32); H-3→L+5 (28.40); H-1→L+5 (4.26); H-1→L+8 (7.43)
T_{18}	H-5→L+1 (15.82); H-5→L+3 (7.58); H-5→L+6(16.69); H-5→L+7 (5.10); H-2→L+3 (3.43); H-2→L+6 (8.39); H-2→L+7 (22.72); H→L+7 (4.03); H→L+10 (5.95)
T_{19}	H-11→L (7.57); H-7→L (3.93); H-6→L (52.30); H-1→L (9.59); H-1→L+5 (8.73)
T_{20}	H-10→L+1 (6.57); H-5→L+1 (3.26); H-4→L+1 (52.04); H→L+1 (7.36); H→L+6 (3.48); H→L+7 (8.83)

Table S6. Calculated singlet and triplet excited states transition configurations of i-PXT-BPin monomer by TD-DFT method (Only the ratio of transition configurations exceed 3% are given).

Energy level	Transition configuration (%)
S_1	H→L (82.11); H→L+2 (4.76); H→L+4 (4.87)
T_1	H-2→L (4.12); H-2→L+3 (4.93); H-1→L (3.84); H-1→L+2 (3.24); H→L (69.23); H→L+2 (3.35)
T_2	H-3→L+2 (10.35); H-2→L (17.34); H-1→L (4.37); H-1→L+1 (10.06); H→L+1 (4.46); H→L+2 (19.81); H→L+3 (23.62)
T_3	H-2→L+2 (5.52); H→L (5.32); H→L+1 (72.05); H→L+2 (5.30)
T_4	H-2→L+1 (11.99); H-1→L+1 (7.75); H→L+1 (3.52); H→L+2 (49.19); H→L+3 (14.36)
T_5	H-3→L (11.82); H-3→L+1 (11.12); H-1→L (27.79); H-1→L+2 (18.98); H→L (9.69); H→L+4 (5.22)
T_6	H-3→L+1 (8.82); H-3→L+2 (15.10); H-2→L (3.86); H-2→L+2 (4.44); H-1→L (9.53); H-1→L+1 (17.47); H-1→L+2 (12.44); H→L+3 (20.71)
T_7	H-3→L+1 (3.72); H-2→L+1 (4.45); H-1→L (8.52); H-1→L+1 (7.45); H-1→L+2 (15.58); H→L+4 (41.63)
T_8	H-3→L (6.56); H-3→L+1 (3.69); H-3→L+3 (6.80); H-1→L (17.62); H-1→L+1 (19.35); H-1→L+3 (6.26); H→L+4 (22.76)
T_9	H-3→L (23.90); H-3→L+1 (4.76); H-3→L+2 (3.27); H-3→L+3 (9.66); H-1→L (4.53); H-1→L+2 (3.86); H-1→L+3 (31.89); H→L+3 (3.59); H→L+4 (4.48)
T_{10}	H-3→L (8.60); H-2→L (41.42); H→L (3.81); H→L+2 (3.70); H→L+3 (14.83); H→L+6 (4.94)
T_{11}	H-5→L+1 (3.00); H-2→L (4.81); H-2→L+2 (5.18); H→L+6 (33.42); H→L+7 (7.22); H→L+8 (11.76); H→L+10 (5.77)
T_{12}	H-5→L (13.68); H-5→L+2 (5.30); H-3→L+2 (7.82); H-2→L+1 (5.18); H-2→L+2 (24.59); H-2→L+3 (8.69); H→L (4.13); H→L+2 (4.27); H→L+4 (3.43)
T_{13}	H-5→L+1 (5.96); H-5→L+2 (4.43); H-3→L+1 (8.44); H-2→L+1 (33.40); H-2→L+2 (12.02); H→L+1 (3.70); H→L+2 (5.89); H→L+3 (3.26)
T_{14}	H-4→L (61.10); H-4→L+2 (7.86); H-4→L+3 (5.23); H-4→L+13 (5.76)
T_{15}	H-5→L (5.08); H-5→L+1 (7.98); H-5→L+3 (3.06); H-3→L+3 (4.71); H-2→L+1 (10.16); H-2→L+2 (3.65); H-2→L+3 (29.45); H→L+1 (3.53); H→L+3 (8.00)
T_{16}	H-8→L (7.44); H-3→L (31.89); H-2→L (7.10); H-1→L (10.40); H-1→L+2 (8.97); H-1→L+3 (14.14)
T_{17}	H-3→L+2 (9.20); H-3→L+3 (6.93); H-2→L+2 (4.75); H-1→L+2 (11.08); H-1→L+3 (7.40); H-1→L+4 (31.62); H→L+4 (4.12)
T_{18}	H-8→L (26.03); H-8→L+2 (5.10); H-3→L+2 (9.85); H-2→L+2 (4.67); H-1→L+1 (8.22); H-1→L+3 (4.18); H-1→L+4 (15.46)
T_{19}	H-20→L (4.36); H-8→L (20.74); H-7→L (16.39); H-5→L (10.30); H-3→L+2 (11.68); H-1→L+1 (6.75)
T_{20}	H-8→L (12.27); H-7→L (13.81); H-5→L (13.85); H-3→L+1 (12.71); H-3→L+2 (3.08); H-2→L+1 (5.01); H-2→L+2 (3.37); H-1→L+1 (3.87); H-1→L+2 (6.80); H-1→L+3 (3.20)

Table S7. Calculated singlet and triplet excited states transition configurations of i-PXT-BPin trimer by TD-DFT method (Only the ratio of transition configurations exceed 3% are given).

Energy level	Transition configuration (%)
S_1	H→L+1 (12.87); H→L+2 (75.59)
T_1	H-7→L+11 (4.63); H-3→L+8 (3.18); H→L+1 (10.91); H→L+2 (64.18); H→L+8 (3.43)
T_2	H-10→L+9 (5.06); H-5→L+4 (3.53); H-2→L (73.59); H-2→L+4 (3.53)
T_3	H-6→L+10 (4.27); H-4→L+1 (4.03); H-4→L+7 (3.21); H-1→L+1 (57.21); H-1→L+2 (9.50); H-1→L+5 (5.46)
T_4	H-11→L+4 (4.43); H-10→L (12.42); H-5→L (5.27); H-5→L+3 (4.57); H-5→L+4 (3.00); H-2→L+3 (30.46); H-2→L+9 (21.38)
T_5	H-9→L+8 (9.13); H-7→L+2 (3.93); H-3→L+6 (7.02); H→L+6 (28.98); H→L+8 (11.36); H→L+11 (18.00)
T_6	H-8→L+7 (10.60); H-6→L+1 (10.94); H-4→L+1 (5.50); H-4→L+5 (7.61); H-1→L+5 (4.80); H-1→L+7 (26.08); H-1→L+10 (20.53)
T_7	H-10→L (3.87); H-10→L+3 (3.70); H-10→L+4 (3.33); H-2→L (4.35); H-2→L+3 (35.60); H-2→L+4 (31.07); H-2→L+9 (4.28)
T_8	H-7→L+2 (4.08); H-7→L+8 (4.50); H→L+2 (3.09); H→L+6 (47.59); H→L+8 (26.08)
T_9	H-6→L+7 (3.37); H-1→L+1 (6.60); H-1→L+5 (71.74); H-1→L+7 (3.96)
T_{10}	H-10→L+3 (11.72); H-5→L+3 (11.72); H-5→L+3 (5.44); H-2→L+4 (45.17); H-2→L+9 (12.80)
T_{11}	H-7→L+6 (12.72); H-3→L+6 (7.32); H→L+6 (8.20); H→L+8 (41.25); H→L+11 (18.11)
T_{12}	H-8→L+5 (3.25); H-6→L+5 (7.49); H-6→L+7 (4.45); H-6→L+10 (3.32); H-4→L+5 (7.53); H-1→L+7 (46.50); H-1→L+10 (16.70);
T_{13}	H-11→L (6.97); H-11→L+3 (8.73); H-10→L+3 (3.26); H-5→L (14.43); H-5→L+3 (4.90); H-5→L+4 (34.42); H-2→L (8.09)
T_{14}	H-8→L+1 (8.71); H-8→L+5 (7.34); H-6→L+5 (7.55); H-4→L+1 (19.63); H-4→L+1 (3.17); H-4→L+5 (3.39); H-4→L+7 (20.87); H-1→L+1 (7.91); H-1→L+10 (4.44)
T_{15}	H-9→L+2 (7.49); H-9→L+6 (11.79); H-7→L+6 (4.27); H-3→L+1 (3.13); H-3→L+2 (17.74); H-3→L+8 (31.31); H→L+2 (6.72); H→L+14 (3.28)
T_{16}	H-12→L+3 (3.45); H-11→L+3 (12.96); H-11→L+4 (4.86); H-10→L (5.81); H-10→L+4 (4.45); H-5→L+3 (19.55); H-2→L+9 (23.24)
T_{17}	H-9→L+6 (9.04); H-9→L+8 (10.17); H-7→L+2 (4.31); H-7→L+8 (5.72); H-3→L+2 (9.62); H-3→L+6 (24.79); H→L+11 (22.88)
T_{18}	H-8→L+5 (4.46); H-8→L+7 (15.36); H-6→L+1 (3.53); H-6→L+7 (8.29); H-4→L+1 (5.14); H-4→L+7 (15.90); H-1→L+10 (22.42)
T_{19}	H-3→L+2 (5.03); H-3→L+8 (11.28); H→L+14 (55.12)
T_{20}	H-5→L (11.30); H-5→L+4 (10.34); H-2→L+12 (55.44)

Table S8. Calculated singlet and triplet excited states transition configurations of TE-BPin monomer by TD-DFT method (Only the ratio of transition configurations exceed 3% are given).

Energy level	Transition configuration (%)
S_1	H→L (81.73); H→L+1 (8.87)
T_1	H-2→L (11.05); H-1→L (3.22); H-1→L+3 (3.22); H→L (64.23)
T_2	H-3→L+2 (4.04); H-3→L+3 (4.00); H-2→L (7.90); H-2→L+1 (6.87); H-2→L+2 (3.37); H-1→L+1 (4.78); H-1→L+2 (6.08); H→L+1 (26.81); H→L+2 (20.98); H→L+3 (5.08)
T_3	H-3→L (15.07); H-3→L+1 (6.35); H-1→L (48.80); H-1→L+3 (3.72); H→L (10.20); H→L+1 (4.00)
T_4	H-3→L+3 (3.08); H-2→L+3 (9.13); H-1→L (8.08); H-1→L+3 (4.35); H→L (3.85); H→L+1 (33.84); H→L+2 (12.50); H→L+3 (12.05)
T_5	H-3→L+3 (3.94); H-2→L+1 (3.85); H-2→L+2 (6.81); H-1→L+1 (16.68); H→L+2 (28.63); H→L+3 (20.66)
T_6	H-3→L+1 (7.64); H-3→L+2 (16.72); H-3→L+3 (5.13); H-1→L+1 (7.39); H-1→L+2 (19.92); H-1→L+3 (12.21); H→L+1 (8.07); H→L+2 (7.63)
T_7	H-3→L+3 (8.12); H-2→L+1 (6.90); H-1→L (10.11); H-1→L+1 (19.12); H-1→L+3 (7.78); H→L+3 (32.49)
T_8	H-3→L (11.44); H-3→L+1 (14.83); H-1→L+1 (8.84); H-1→L+2 (25.68); H-1→L+3 (16.65); H→L+1 (3.49); H→L+2 (6.33); H→L+4 (3.17)
T_9	H-3→L+2 (4.35); H-1→L+7 (8.97); H→L+4 (58.46)
T_{10}	H-6→L (9.34); H-2→L (16.75); H-2→L+2 (7.71); H-2→L+3 (3.72); H-1→L+3 (5.05); H-1→L+4 (15.96); H→L (3.88); H→L+7 (20.14)
T_{11}	H-6→L+1 (4.37); H-2→L (36.47); H-2→L+1 (5.82); H-1→L+4 (7.69); H→L (4.58); H→L+1 (4.51); H→L+2 (7.12); H→L+7 (3.94)
T_{12}	H-5→L (9.45); H-3→L (34.36); H-1→L (12.33); H-1→L+1 (3.92); H-1→L+2 (5.43); H→L+6 (9.72)
T_{13}	H-6→L (5.23); H-2→L+1 (23.96); H-2→L+2 (12.04); H-1→L+4 (17.72); H→L (5.05); H→L+7 (5.51)
T_{14}	H-5→L (4.58); H-2→L+3 (4.66); H-1→L (3.92); H→L+6 (45.38); H→L+8 (9.53)
T_{15}	H-6→L+2 (4.07); H-5→L (4.08); H-5→L+1 (4.15); H-5→L+2 (3.13); H-3→L+1 (6.46); H-3→L+2 (6.78); H-2→L+1 (8.13); H-2→L+2 (11.44); H-2→L+3 (7.73); H-1→L+1 (3.72); H-1→L+2 (3.68); H→L+2 (3.38); H→L+3 (3.64); H→L+4 (7.89)
T_{16}	H-6→L+1 (5.39); H-6→L+3 (4.29); H-2→L+1 (7.54); H-2→L+2 (7.16); H-2→L+3 (27.53); H-1→L+4 (6.21); H→L+1 (4.99); H→L+3 (6.85)
T_{17}	H-6→L+2 (3.38); H-5→L (3.82); H-5→L+1 (7.47); H-4→L (3.35); H-3→L+1 (7.61); H-3→L+2 (4.51); H-3→L+3 (4.50); H-2→L+1 (5.59); H-2→L+2 (14.17); H-2→L+3 (6.03); H-1→L+1 (7.96); H→L+2 (4.13); H→L+3 (3.48); H→L+6 (4.86)
T_{18}	H-4→L (65.53); H-4→L+1 (3.88); H-4→L+13 (3.90)
T_{19}	H-5→L+1 (8.33); H-5→L+2 (8.47); H-3→L+2 (3.97); H-3→L+3 (16.74); H-2→L+3 (3.09); H-1→L+1 (7.39); H-1→L+2 (15.30); H-1→L+6 (12.93); H-1→L+8 (3.16)
T_{20}	H-5→L+3 (10.43); H-3→L+1 (19.33); H-3→L+2 (12.30); H-1→L+2 (4.19); H-1→L+3 (33.14)

Table S9. Calculated singlet and triplet excited states transition configurations of TE-BPin dimer by TD-DFT method (Only the ratio of transition configurations exceed 3% are given).

Energy level	Transition configuration (%)
S_1	H-1→L (79.20); H-1→L+2 (7.63); H-1→L+3 (5.09)
T_1	H-6→L (13.36); H-3→L+4 (3.12); H-1→L (62.12)
T_2	H-4→L+1 (12.07); H-2→L+7 (4.38); H→L+1 (62.14)
T_3	H-7→L+4 (5.20); H-6→L (4.32); H-6→L+2 (5.53); H-6→L+3 (8.06); H-3→L+2 (6.51); H-3→L+4 (3.29); H-1→L+2 (14.36); H-1→L+3 (38.21)
T_4	H-5→L+6 (3.54); H-5→L+7 (3.56); H-4→L+1 (6.29); H-4→L+5 (8.41); H-4→L+6 (4.11); H-2→L+5 (5.60); H-2→L+6 (5.01); H→L+5 (26.17); H→L+6 (25.46)
T_5	H-6→L+4 (10.36); H-3→L+4 (4.36); H-1→L (9.89); H-1→L+2 (46.70); H-1→L+3 (9.20); H-1→L+4 (4.18)
T_6	H-4→L+7 (10.71); H-2→L+7 (5.63); H→L+1 (8.85); H→L+5 (36.98); H→L+6 (20.60); H→L+7 (5.35)
T_7	H-7→L (15.46); H-3→L (57.24); H-1→L (4.27); H-1→L+4 (7.10)
T_8	H-5→L+1 (12.58); H-2→L+1 (58.18); H→L+7 (12.36)
T_9	H-7→L+4 (3.77); H-6→L+2 (5.94); H-6→L+3 (3.67); H-3→L+2 (16.71); H-1→L+2 (4.49); H-1→L+3 (13.16); H-1→L+4 (31.25)
T_{10}	H-5→L+1 (4.76); H-5→L+7 (6.47); H-4→L+5 (4.37); H-4→L+6 (5.30); H-2→L+5 (16.22); H-2→L+7 (6.42); H→L+1 (5.18); H→L+6 (18.00); H→L+7 (22.58)
T_{11}	H-12→L+4 (3.03); H-7→L+2 (10.78); H-7→L+3 (6.58); H-7→L+4 (9.46); H-3→L+2 (11.76); H-3→L+3 (9.34); H-3→L+4 (18.67); H-1→L+2 (7.02); H-1→L+3 (11.40)
T_{12}	H-5→L+5 (11.01); H-5→L+6 (13.57); H-5→L+7 (4.49); H-2→L+5 (11.21); H-2→L+6 (17.11); H-2→L+7 (10.00); H→L+5 (10.99); H→L+6 (5.95)
T_{13}	H-7→L+2 (4.83); H-7→L+3 (3.27); H-7→L+4 (5.98); H-6→L+2 (6.44); H-3→L (11.72); H-3→L+2 (14.92); H-3→L+4 (11.23); H-1→L+2 (3.11); H-1→L+4 (25.39)
T_{14}	H-5→L+6 (4.15); H-5→L+7 (7.47); H-4→L+5 (5.70); H-2→L+1 (12.09); H-2→L+5 (13.57); H-2→L+7 (13.82); H→L+7 (29.64)
T_{15}	H-7→L (7.12); H-7→L+2 (9.00); H-7→L+3 (5.59); H-3→L+2 (8.79); H-3→L+3 (45.91); H-3→L+4 (3.60); H-1→L+2 (4.79)
T_{16}	H-5→L+1 (9.61); H-5→L+5 (11.91); H-2→L+5 (14.37); H-2→L+6 (34.29); H-2→L+7 (8.72); H→L+5 (4.28); H→L+6 (4.89)
T_{17}	H-13→L (3.19); H-12→L (4.97); H-7→L+3 (5.84); H-6→L (14.16); H-3→L+12 (6.05); H-1→L+8 (9.78); H-1→L+9 (6.21)
T_{18}	H-9→L+1 (5.03); H-5→L+6 (5.38); H-4→L+1 (6.90); H-2→L+15 (8.22); H→L+10 (46.02)
T_{19}	H-13→L (6.91); H-6→L (13.04); H-6→L+3 (12.60); H-3→L+4 (3.97); H-3→L+8 (6.26); H-1→L (3.69); H-1→L+8 (13.31); H-1→L+9 (4.18); H-1→L+12 (12.70)
T_{20}	H-11→L+1 (7.80); H-4→L+1 (10.68); H-4→L+6 (13.42); H-2→L+7 (5.00); H-2→L+10 (12.79); H→L+1 (3.31); H→L+10 (6.63); H→L+15 (16.99)

6. Single Crystals Information

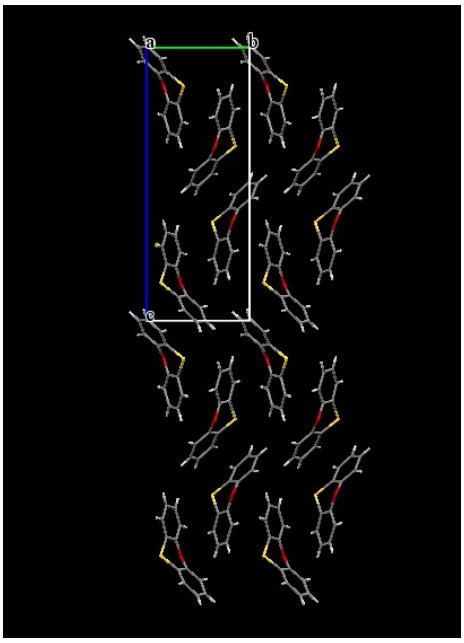

Fig. S11 Single crystal structure of PXT along a-axis in a 2×2×2 packing diagram.

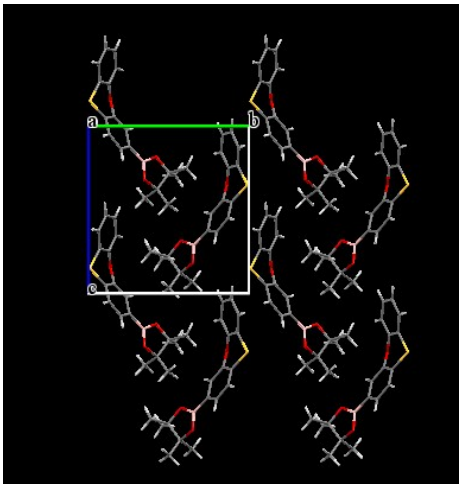

Fig. S12 Single crystal structure of PXT-BPin along a-axis in a 2×2×2 packing diagram.

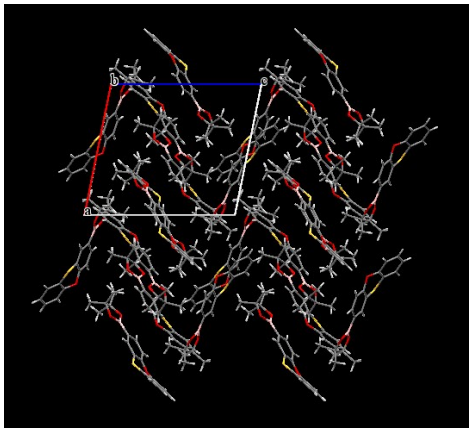

Fig. S13 Single crystal structure of i-PXT-BPin along b-axis in a 2×2×2 packing diagram.

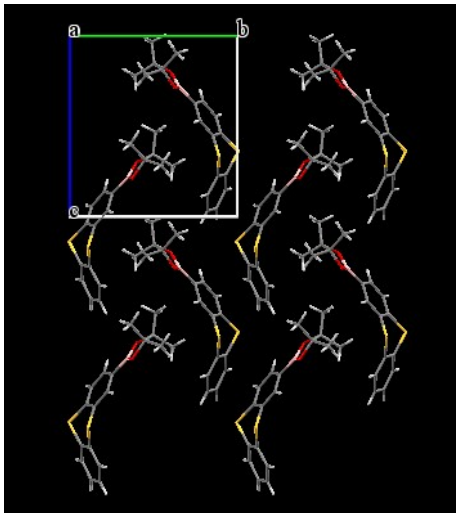

Fig. S14 Single crystal structure of TE-BPin along a-axis in a 2×2×2 packing diagram.

Table S10 Detailed information of PXT, TE-BPin, PXT-BPin and i-PXT-BPin single crystals [a]

Name	PXT	TE-BPin	PXT-BPin	i-PXT-BPin
Formula	$C_{12}H_8OS$	$C_{18}H_{19}BO_2S_2$	$C_{18}H_{19}BO_3S$	$C_{18}H_{19}BO_3S$
Space Group	P 2_1 2_1 2_1	P n	P n	P -1
Cell Lengths	a 5.8619 (2)	a 6.46310 (10)	a 6.03420 (9)	a 13.17231 (19)
(Å)	b 7.6914 (3)	b 10.9896 (2)	b 11.41823 (12)	b 13.1966 (2)
	c 20.4081 (7)	c 11.8559 (3)	c 11.96434 (12)	c 15.79206 (15)
Cell Angles	α 90	α 90	α 90	α 111.0153 (13)
(°)	β 90	β 90.511 (2)	β 96.3702 (10)	β 97.9913 (11)
	γ 90	γ 90	γ 90	γ 97.2811 (13)
Cell Volume	920.124	842.054	819.252	2490.92
($Å^3$)				
Z	4	2	2	11

[a]All crystal structures have been deposited at the Cambridge Crystallographic Data Centre and the allocated deposition numbers are 1877801 (PXT), 1877800 (PXT-BPin), 1877802 (i-PXT-BPin) and 1877803 (TE-BPin).

7. Notes and Reference

1. Gaussian 09, Revision B.01, M. J. Frisch, G. W. Trucks, H. B. Schlegel, G. E. Scuseria, M. A. Robb, J. R. Cheeseman, G. Scalmani, V. Barone, G. A. Petersson, H. Nakatsuji, X. Li, M. Caricato, A. Marenich, J. Bloino, B. G. Janesko, R. Gomperts, B. Mennucci, H. P. Hratchian, J. V. Ortiz, A. F. Izmaylov, J. L. Sonnenberg, D. Williams-Young, F. Ding, F. Lipparini, F. Egidi, J. Goings, B. Peng, A. Petrone, T. Henderson, D. Ranasinghe, V. G. Zakrzewski, J. Gao, N. Rega, G. Zheng, W. Liang, M. Hada, M. Ehara, K. Toyota, R. Fukuda, J. Hasegawa, M. Ishida, T. Nakajima, Y. Honda, O. Kitao, H. Nakai, T. Vreven, K. Throssell, J. A. Montgomery, Jr., J. E. Peralta, F. Ogliaro, M. Bearpark, J. J. Heyd, E. Brothers, K. N. Kudin, V. N. Staroverov, T. Keith, R. Kobayashi, J. Normand, K. Raghavachari, A. Rendell, J. C. Burant, S. S. Iyengar, J. Tomasi, M. Cossi, J. M. Millam, M. Klene, C. Adamo, R. Cammi, J. W. Ochterski, R. L. Martin, K. Morokuma, O. Farkas, J. B. Foresman, and D. J. Fox, Gaussian, Inc., Wallingford CT, 2016.
2. A. D. Becke, *Phys. Rev. A,* 1988, **38**, 3098.
3. Y. Zhao, D. G. Truhlar, *J. Phys. Chem. A*, 2004, **108**, 6908.